FEBS Letters

FEBS PRESS science publishing by scientists

Reciprocal regulation between mRNA and microRNA enables a bistable switch that directs cell fate decisions

Xiao-Jun Tian[1], Hang Zhang[2], Jingyu Zhang[1] and Jianhua Xing[1,3]

1 Department of Computational and Systems Biology, School of Medicine, University of Pittsburgh, PA, USA
2 Genetics, Bioinformatics and Computational Biology Program, Virginia Polytechnic Institute and State University, Blacksburg, VA, USA
3 Computational Science Research Center, Beijing, China

Correspondence
X.-J. Tian or J. Xing, Department of Computational & Systems Biology, School of Medicine, University of Pittsburgh, 3501 Fifth Avenue, Pittsburgh, PA 15213, USA
Fax: +1 412 648 3163
Tel: +1 412 648 0174; +1 412 383 5743
E-mails: xjtian@pitt.edu; xing1@pitt.edu

(Received 27 July 2016, revised 21 August 2016, accepted 22 August 2016, available online 18 September 2016)

doi:10.1002/1873-3468.12379

Edited by Tamas Dalmay

Micro RNAs (miRNAs) serve as crucial post-transcriptional regulators in a variety of essential cell fate decisions. However, the contribution of mRNA–miRNA mutual regulation to bistability is not fully understood. In the present study, we built a set of mathematical models of mRNA–miRNA interactions and systematically analyzed the sensitivity of the response curves under various conditions. Our findings indicate that mRNA–miRNA reciprocal regulation could manifest ultrasensitivity to subserve the generation of bistability when equipped with a positive feedback loop. We also find that the region of bistability is expanded by a stronger competing endogenous mRNA. Interestingly, bistability can be generated without a feedback loop if multiple miRNA binding sites exist on a target mRNA. Thus, we demonstrate the importance of simple mRNA–miRNA reciprocal regulation in cell fate decisions.

Keywords: bistability; cell fate decision; ceRNA; reciprocal regulation; recycle ratio; ultrasensitivity

MicroRNAs (miRNAs) are small noncoding RNA molecules containing approximately 22 nucleotides that exist ubiquitously in many living organisms for post-transcriptional regulation of gene expression. Growing studies reveal that miRNAs are essential in various essential cell fate decision processes, such as pluripotency and reprogramming [1], epithelial-to-mesenchymal transition [2], cancer stem cells [3] and metastasis [4]. Cells make a choice between two alternative fates: either with a high/low level of mRNA/miRNA or with the opposite expression pattern. The dysregulation of miRNAs is correlated with pathological conditions such as cancer development, as well as cardiovascular and metabolic diseases. During the last decade, studies have accumulated with respect to the basic molecular mechanisms of miRNA biogenesis, function and degradation [5]. With recent quantitative measurements on miRNA dynamics using techniques such as quantitative fluorescence microscopy [6], there is now a timely and urgent need to perform systematic mathematical analysis on mRNA–miRNA mutual regulation and its effect on gene regulatory network dynamics.

As a result of base-pairing interactions, miRNA inhibits its target mRNA through two modes: translational repression and mRNA degradation [7]. The degree of sequence complementarity between miRNA and mRNA determines the mode of mRNA silencing [8]. Extensive complementarity, which often occurs in plants, induces cleavage and degradation of the target mRNA [9,10]. Partial complementarity, which occurs between the vast majority of miRNAs and their target mRNA in metazoans, results in translational repression or degradation [7]. In addition, under some circumstances, miRNA can stimulate the translation of mRNA through an Argonaute/FMR1-mediated

Abbreviations
ceRNA, competing endogenous mRNA; ceRNET, ceRNA network; miRNA, micro RNA.

mechanism [11]. Interestingly, miRNA can establish a threshold of target mRNA [6].

In reverse, mRNA targets reciprocally control the stability and function of miRNAs [11–13]. Target interaction can stabilize miRNA by preventing its release from Argonaute, with subsequent destabilization [14]. The miRNAs in a mRNA–miRNA complex may be either degraded together with the mRNA with extensive complementarity [15–17] or be recycled [18]. Furthermore, each miRNA may target tens to hundreds of mRNAs [19,20], enabling cross-talk between competing endogenous RNAs (ceRNAs) targeted by the same miRNA [21]. Consequently, the reciprocal regulation between miRNAs and their targets adds a significant level of complexity to the mRNA–miRNA relationships.

Given the prevalent involvement of the mRNA–miRNA interaction in cell fate decision processes, extensive efforts have been made to determine the thermodynamic standard free energy of binding between mRNAs and miRNAs ΔG^0, and several computational tools are available for *in silico* prediction [19]. Figure 1A shows the distribution of the standard free energy of binding between miR-34a and mRNAs of 354 human genes calculated using PICTAR [22]. Notably, different mRNAs may have the same ΔG^0. Figure 1B gives four such examples. These mRNAs, with only one miR-34a binding site, form complexes with miR-34a that have drastically different configurations and a number of complementary base pairs. It is questionable whether these mRNAs, even under the same conditions (e.g. concentrations of involved molecular species), undergo the same miR-34a mediated regulation kinetics. On the other hand, miR-34a shows differing positive feedback with respect to its targets, such as miR-34/snail1 [23], miR-34a/SIRT1/p53 [24] and miR-34a/IL-6R/STAT3 [25] (Fig. 1C). Moreover, these mRNA–miRNA feedback loops play important roles in cell fate decisions, such as miR-34/snail1 in the partial epithelial-to-mesenchymal transition [26,27]. However, the contribution of ultrasensitivity from mRNA–miRNA reciprocal regulation to bistability is controversial [27–32]. Thus, there is an urgent need to explore the critical roles of the mRNA–miRNA mutual interaction in the cell fate decision in a general model.

In the present study, we use mathematical and computational analysis to demonstrate the critical role of the mRNA–miRNA mutual interaction in cell fate decisions. We find that the reciprocal regulation between mRNA and miRNA is either ultrasensitive or subsensitive, and either inhibitive or protective. Ultrasensitivity from the mRNA–miRNA reciprocal regulation contributes to bistability generation when it is equipped with a positive feedback loop. Furthermore, the region of bistability is expanded when a stronger competitor (ceRNA) is involved because the degree of response sensitivity is amplified. Alternatively, bistability can be generated from the mRNA–miRNA reciprocal interaction when there is more than one miRNA binding site on the target mRNA.

Methods

Model of mRNA–miRNA reciprocal regulation

Figure 2A summarizes all possible scenarios of mRNA–miRNA reciprocal regulation. miRNAs either suppress an mRNA through translational repression or accelerated degradation, or activate an mRNA through stimulated translation. In reverse, an mRNA either suppresses an miRNA through accelerated degradation, or activates an miRNA by sequestering it from degradation. To analyze the contribution of ultrasensitivity from the mRNA–miRNA reciprocal regulation to the generation of bistability, an inhibition arm in which the protein product of mRNA inhibits the synthesis of miRNA can be added to enclose a double-negative feedback loop (Fig. 2B).

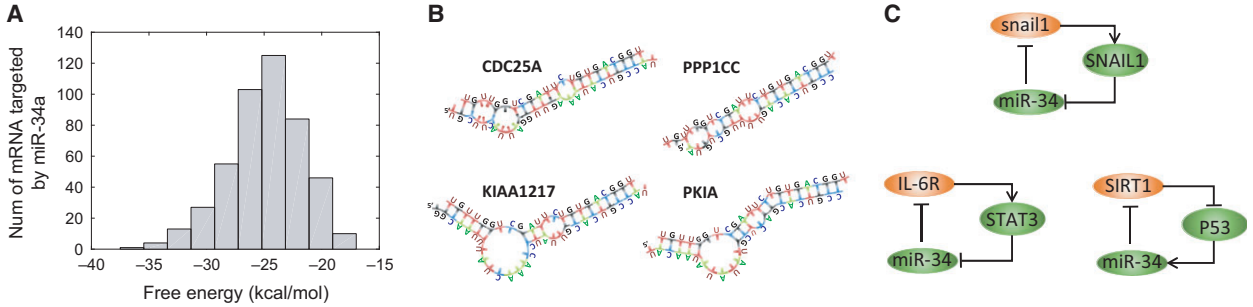

Fig. 1. Target prediction of miR-34a using PICTAR [22]. (A) Distribution of standard free energy of binding between miR-34a and targeting mRNAs. (B) Examples of predicted mRNA–miRNA complex configurations for different target mRNAs with the same ΔG^0 but a different number of complementary base pairs. (C) Examples of miR-34a mediated positive feedback loops.

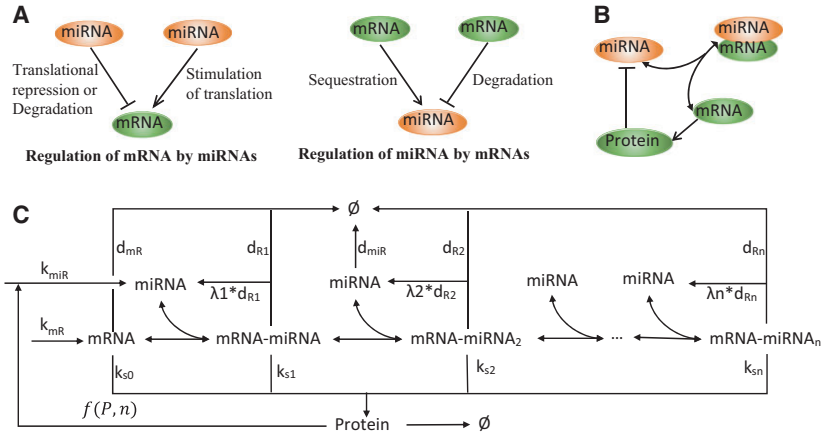

Fig. 2. Mathematical model set-up. (A) Reported possible mRNA–miRNA reciprocal regulations. (B) Positive feedback motif, in which miRNA and mRNA regulate each other through base-pairing interactions, whereas the protein product of mRNA inhibits the transcription of miRNA by binding to its promoter. (C) Kinetic schemes for mRNA–miRNA interaction with multiple miRNA binding sites in the sequence of mRNA. A positive feedback loop can be formed if protein inhibits the transcription of miRNA.

Figure 2C shows the corresponding kinetic schemes for an mRNA with N miRNA binding sites. There are $C_N^i = N!/(i!(N-i)!)$ different complexes that consist of one mRNA and $i(\leq N)$ copies of miRNA.

Noting that the binding/unbinding events between miRNAs and mRNAs are typically much faster than other processes, such as transcription, translation and degradation. We assume that the binding/unbinding processes can be approximated as being in quasi-equilibrium. With no detailed information on cooperativity of mRNA–miRNA binding, we assume that each miRNA binds to the mRNA independently, and the binding free energy for each binding site is the same (ΔG^0). Then, each form of the mRNA–miRNA$_i$ complex (R_i) has the same level, denoted as $[R_i]$, and the total level of the mRNA–miRNA$_i$ complex is $C_N^i[R_i]$. Furthermore, the levels of free miRNA and mRNA ([miR], [mR]), the total levels of miRNA and mRNA ($[\mathrm{miR}]_t$, $[\mathrm{mR}]_t$) and the mRNA–miRNA$_i$ complex $[R_i]$ are constrained as below,

$$[\mathrm{mR}] = [\mathrm{mR}]_t - \sum_{i=1}^{N} C_N^i [R_i] \tag{1}$$

$$[\mathrm{miR}] = [\mathrm{miR}]_t - \sum_{i=1}^{N} i C_N^i [R_i] \tag{2}$$

Under the quasi-equilibrium approximation, the following relationship exists between $[R_i]$ and $[R_{i-1}]$:

$$K_i[\mathrm{miR}][R_{i-1}] = [R_i], \quad i = 1 \ldots N \tag{3}$$

where [miR] is the cellular level of the free miRNA under study, $[R_0]$ is defined as the mRNA concentration [mR] and $K = \exp(-\Delta G^0)$ is the binding constant. Here, ΔG^0 is in the unit of k_{BT}, the product of Boltzmann's constant and temperature. The degradation rate constant of $[R_i]$ is d_{Ri} and the translation rate of the $[R_i]$ is k_{si}. Upon degradation of the complex mRNA–miRNA$_i$, miRNA molecules can be recycled with a ratio λ_i ($(0 \leq \lambda_i \leq 1)$). Thus, the equations of total level of miRNA, mRNA and protein [P] are:

$$\frac{\mathrm{d}[\mathrm{miR}]_t}{\mathrm{d}t} = \frac{k_{\mathrm{miR}}}{(1 + F * ([\mathrm{P}]/J)^n)} - d_{\mathrm{miR}}[\mathrm{miR}] - \sum_{i=1}^{N} (1 - \lambda_i) i C_N^i d_{Ri} [R_i] \tag{4}$$

$$\frac{\mathrm{d}[\mathrm{mR}]_t}{\mathrm{d}t} = k_{\mathrm{mR}} - d_{\mathrm{mR}}[\mathrm{mR}] - \sum_{i=1}^{N} C_N^i d_{\mathrm{Ri}} [R_i] \tag{5}$$

$$\frac{\mathrm{d}[\mathrm{P}]}{\mathrm{d}t} = k_{s0}[\mathrm{mR}] + \sum_{i=1}^{N} k_{si} C_N^i [R_i] - d_p[\mathrm{P}] \tag{6}$$

For convenience in subsequent discussions, we reform the above equations as:

$$\tau_{\mathrm{miR}} \frac{\mathrm{d}[\mathrm{miR}]_t}{\mathrm{d}t} = \frac{\alpha_{\mathrm{miR}}}{(1 + F * ([\mathrm{P}]/J)^n)} - [\mathrm{miR}] - \sum_{i=1}^{N} (1 - \lambda_i) i C_N^i \beta_{\mathrm{Ri}} [R_i] \tag{7}$$

$$\tau_{\mathrm{mR}} \frac{\mathrm{d}[\mathrm{mR}]_t}{\mathrm{d}t} = \alpha_{\mathrm{mR}} - [\mathrm{mR}] - \sum_{i=1}^{N} C_N^i \beta_{\mathrm{Ri}} [R_i] \tag{8}$$

$$\tau_{\mathrm{P}} \frac{\mathrm{d}[\mathrm{P}]}{\mathrm{d}t} = \alpha_{\mathrm{P0}}[\mathrm{mR}] + \sum_{i=1}^{N} \alpha_{\mathrm{P}i} C_N^i [R_i] - [\mathrm{P}] \tag{9}$$

where, $\tau_{\mathrm{miR}} = 1/d_{\mathrm{miR}}$, $\tau_{\mathrm{mR}} = 1/d_{\mathrm{mR}}$, $\tau_{\mathrm{P}} = 1/d_{\mathrm{P}}$, $\alpha_{\mathrm{miR}} = k_{\mathrm{miR}}/d_{\mathrm{miR}}$, $\alpha_{\mathrm{mR}} = k_{\mathrm{mR}}/d_{\mathrm{mR}}$, $\beta_{\mathrm{Ri}} = d_{\mathrm{Ri}}/d_{\mathrm{mR}}$, $\alpha_{\mathrm{P0}} = k_{s0}/d_{\mathrm{p}}$ and $\alpha_{\mathrm{P}i} = k_{\mathrm{si}}/d_{\mathrm{p}}$. The values of τ_{miR}, τ_{miR} and τ_{miR} indicate the time scale of miRNA, mRNA and protein, respectively; the values of α_{miR}, α_{mR} and α_{P0} determine the level of miRNA, mRNA and protein without mutual regulation, respectively; and the values of K_i, β_{Ri}, λ_i and $\alpha_{\mathrm{P}i}$ indicate the strength of the inhibition with respect to each other. The parameters values are used as follows, except where specified: $\alpha_{\mathrm{miR}} = 1$,

$\alpha_{mR} = 1$, $\alpha_{P0} = 10$, $\alpha_{Pi} = 1$, $\beta_{Ri} = 5$, $K_i = 10 \sim 100$ and $\lambda_i = 0.5$. Parameters α_{miR} and α_{mR} will used for dose–response curve analysis, whereas the effect of other parameters on the sensitivity analysis will also be systematically analyzed. It is noted that the time scale does not change the steady-state. Thus, the exact values of τ_{miR}, τ_{mR} and τ_P do not affect the conclusion, and so we used $\tau_{miR} = 1$, $\tau_{mR} = 1$ and $\tau_P = 1$. Throughout the present study, all the variables and parameters are provided in arbitrary units.

Bistability analysis

To describe the inhibition of miRNA synthesis by the protein, an inhibitory Hill function $\frac{J^n}{J^n+[P]^n}$ is multiplied to α_{miR} as shown in Eqn (7). The analysis with this positive feedback can be achieved by setting $F = 1$ instead of $F = 0$ in cases without positive feedback. If $n \leq 1$ for the Hill coefficient, this inhibition arm is not ultrasensitive. Therefore, in this model system, the required nonlinearity can come either from protein-mediated inhibition on miRNA synthesis, or directly from the mRNA–miRNA mutual regulation. To demonstrate the contribution of these two sources of ultrasensitivity to bistability, the minimum of the Hill coefficient (n_{min}) to generate bistability will be analyzed. If $n_{min} < 1$, then the bistable system required ultrasensitivity can result from the mRNA–miRNA mutual interaction. The method of determining n_{min} is shown in Fig. S1. First, a one-parameter bifurcation diagram is analyzed to check the bistability and identify the Saddle-node bifurcation points. Then, based on these two Saddle-node bifurcation points, a two-parameter bifurcation diagram is analyzed to identify the cusp bifurcation point, where n_{min} is located.

Sensitivity analysis

The steady-state response curve is often used to describe how the output of the system (O) depends on the input (I). To quantify the sensitivity of the system, the instantaneous sensitivity is defined as the ratio of the fractional changes in response output ($\Delta O/O$) and stimulus input ($\Delta I/I$):

$$s(I) = \lim_{\Delta I \to 0} \frac{\Delta O/O}{\Delta I/I} = \frac{dO/O}{dI/I} = \frac{d\log(O)}{d\log(I)}$$

Instantaneous sensitivity is also known as 'logarithmic gain' in biochemical systems theory [33] or as the 'local sensitivity coefficient' in local parameter sensitivity analysis [34]. The response is ultrasensitive if $|s| > 1$, subsensitive if $0 < |s| < 1$, desensitive if $s = 0$ and linear if $|s| = 1$. The sign of s indicates whether I inhibits or activates O. In general, the instantaneous sensitivity s is not constant but depends on the input (I). We denote the dependence of instantaneous sensitivity s on I as the instantaneous sensitivity curve, and the extremum of this curve as the maximum (in the sense of the absolute value) sensitivity (s_m) of the specific I–O curve. Under this definition, the maximum sensitivity of a Hill function ($\frac{I^n}{I^n+K^n}$) is exactly the Hill coefficient n. Thus, s_m can be used as the gauge of the degree of sensitivity. The steady-state response curves and bifurcation diagrams are constructed using PYDSTOOL [35].

Results

The major aim of the present study is to explore the contribution of ultrasensitivity from mRNA–miRNA mutual regulation to the generation of bistability. We first performed a sensitivity analysis for mRNA–miRNA mutual regulation with a single binding site, and then analyzed the contribution of the ultrasensitivity to bistability with a feedback loop. We also explored the effect of ceRNA on the bistability generation. Lastly, we extend our analysis to multiple binding sites.

The ultrasensitivity from mRNA–miRNA mutual regulation subserves the generation of bistability when equipped with a positive feedback loop

Given that miRNA and mRNA molecules are able to reciprocally regulate each other, we analyzed the contribution of the sensitivity from the mutual regulation to the generation of bistability and cell fate decision. We begin with the case where an mRNA has only one binding site for the miRNA.

First, the sensitivity of regulation of mRNA/protein by miRNA is analyzed. As shown in Fig. 3A, under mode of absence of feedback regulation, the protein concentration decreases with the miRNA synthesis rate constant α_{miR}, reflecting the inhibition of miRNA with respect to mRNA/protein. Most of the response curves are sigmoidal shaped with respect to α_{miR} in logarithmic scale, exhibiting a progression from a weak inhibition that accelerates and approaches total inhibition with an increase of α_{miR}. The sharpness of the sigmoidal shape decreases and eventually disappears when the recycle ratio λ increases. Shape changes of the response curves are also reflected by the corresponding instantaneous sensitivity curves (Fig. 3B), which are bell-shaped with an extremum in the middle, where the mRNA level is most sensitive to the miRNA level change. The maximum sensitivity, s_m, is negative for inhibition and increases with the recycle ratio λ (Fig. 3C). That is, the larger the recycle ratio and the more efficient the miRNA, the less sensitive is the inhibition of mRNA by miRNA. Therefore, ultrasensitivity is generated by sacrificing efficiency with respect to inhibiting mRNA. Notably, when the recycle ratio is

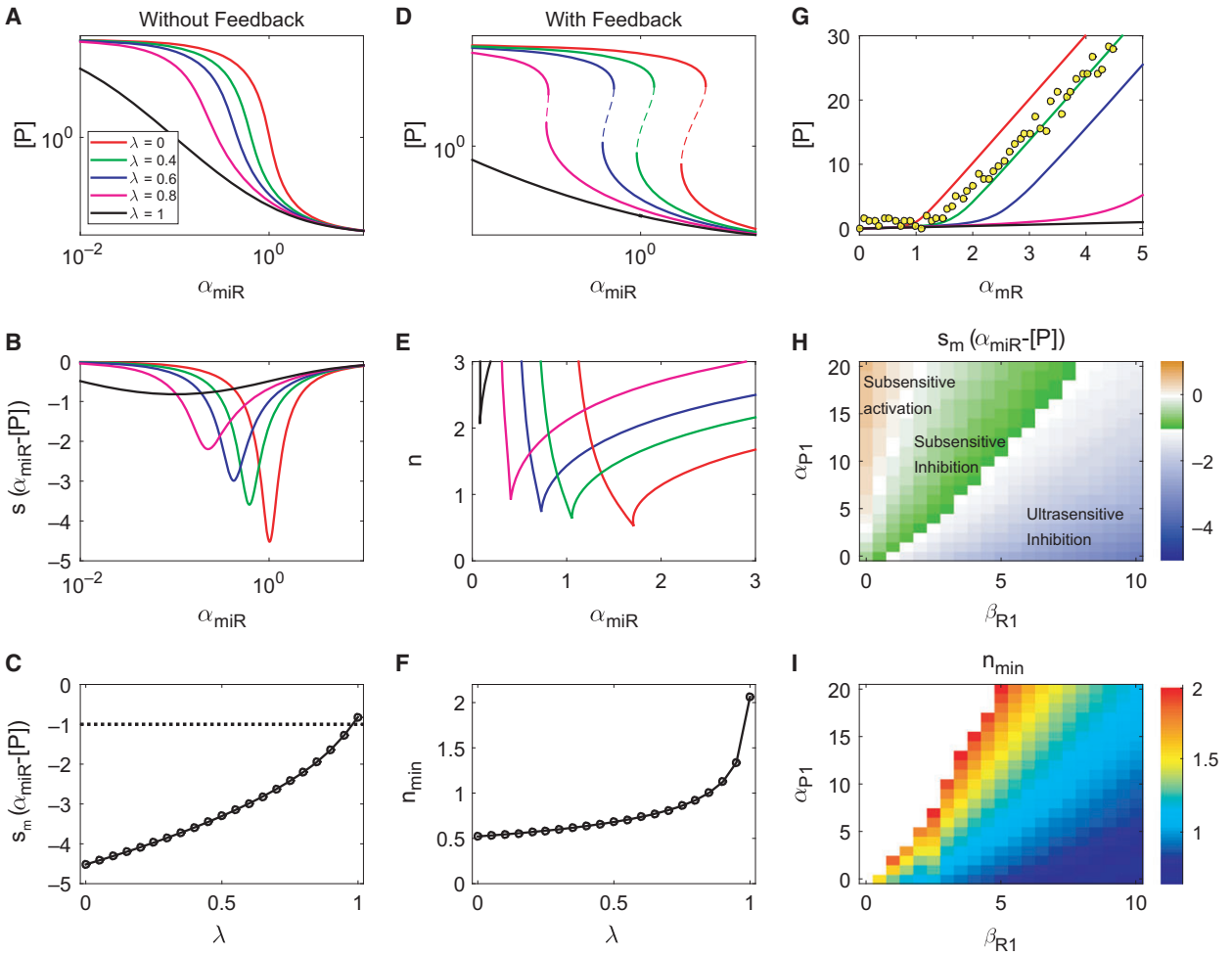

Fig. 3. Sensitivity and bistability analyses of the mRNA–miRNA reciprocal regulation, with one miRNA binding site on mRNA. (A) Dependence of the protein level on the miRNA synthesis rate constant α_{miR} under different values of the recycle ratio λ without a feedback loop. (B) Dependence of the instantaneous sensitivity on α_{miR} under different values of λ. (C) Dependence of the maximum sensitivity s_m of the $\alpha_{miR} - [P]$ response curve on the value of λ. (D) Dependence of the protein level on the miRNA synthesis rate constant α_{miR} under different values of the recycle ratio λ with a feedback loop. Dotted line denotes unstable states. (E) The bistable region in the space of α_{miR} and Hill coefficient n under different values of λ. (F) Dependence of the min Hill coefficient n_{min} for bistability under different values of λ. (G) Dependence of the protein level on the expression rate constant of mRNA α_{mR} under a different recycle ratio λ; also plotted are experimental data (yellow circles) from Mukherji *et al.* [6]. (H) The maximum sensitivity s_m of the $\alpha_{miR}-[P]$ response curve in the parameter space spanned by the mRNA–miRNA complex translation rate constant α_{P1} and the degradation rate constant β_{R1}. (I) The minimal Hill coefficient n_{min} for bistability in the parameter space of α_{P1} and β_{R1}. In the blank region, either n_{min} is larger than 2 or no bistability is found.

near 1, $|s_m|$ is less than 1. That is, regulation of mRNA by miRNA shows subsensitivity instead of ultrasensitivity when the miRNA is almost completely recycled.

A positive feedback loop with an ultrasensitivity arm can produce bistability [36], which plays an essential role in cell fate decisions. We hypothesize that ultrasensitivity from the mRNA–miRNA reciprocal regulation contributes to the generation of bistability. Thus, response curves under the presence of feedback regulation are analyzed. Figure 3D clearly shows the existence of bistable regions of protein level when varying α_{miR}, even when $n = 1$ for the Hill coefficient. The existence of bistability is also demonstrated in Fig. S2. The nullclines of $[mR]_t$ and $[miR]_t$ have three intersection points, two of which are stable-steady states and the other is an unstable steady-state. The two-parameter bifurcation diagrams in Fig. 3E show how the parameter region of bistability changes over n and α_{miR}. As expected, with other parameters fixed, the value of n needs to exceed a critical value to generate bistability. This critical value has a cusp-shaped dependence on α_{miR}, which relates to the bell-shaped

sensitivity curves in Fig. 3B. Notably, this critical value of n can be less than 1 for certain values of α_{miR}. That is, both mRNA–miRNA mutual regulation and protein regulation on miRNA synthesis contribute to the generation of bistability, as long as the composite nonlinearity exceeds a threshold value.

It is noted that the bistable region decreases with the recycle ratio. That is, the miRNA recycle ratio λ also affects the critical value of Hill coefficient n_{min}. Indeed, Fig. 3E shows that the space of λ and the Hill coefficient n is divided into monostable and bistable regions. The smaller the value of λ, the smaller the Hill coefficient n that is required to generate bistability. This is consistent with the results showing that the maximum sensitivity (s_m) of the reciprocal regulation between miRNA and mRNA increases with a decrease in the recycle ratio (Fig. 3C). That is, when miRNA is almost completely recycled, a larger nonlinearity from the other source is required to generate bistability. In general, when the miRNA is not fully recycled, bistability can originate from the synergistic effect of mRNA–miRNA reciprocal regulation and protein–miRNA transcriptional regulation. This conclusion is also confirmed when exploring the dependence of s_m and n_{min} by changing other parameters (Fig. S3). For example, our previous study shown that a double negative feedback loop between Snail1 and miR-34 functions as a bistable switch to control the transition of an epithelial to partial epithelial-to-mesenchymal transition state [26,27]. In this system, snail1 mRNA has only one binding site for miR-34 [23], and the nonlinearity can originate from both Snail1 inhibition of miR-34 transcription (with $n = 2$) and miR-34/snail1 mutual regulation in human [27]. However, in rat/mouse, the nonlinearity originates from miR-34/snail1 mutual regulation because only one Snail1 binding site exists on the miR-34 promoter (with $n = 1$) [23]. That is, the ultrasensitivity from miRNA-mRNA mutual regulation and that from Hill coefficient can compensate each other to generate bistability.

The threshold dynamics is more transparent in Fig. 3G. When plotted against the mRNA synthesis rate constant, α_{mR}, the protein level remains low until α_{mR} exceeds a threshold value so that mRNA molecules escape from miRNA-mediated repression by titrating the miRNA in the system, and the threshold increases with λ. The threshold behavior is consistent with the quantitative measurements of Mukherji *et al.* [6] (Fig. 3G, yellow circles).

Furthermore, the sensitivity of the miRNA regulated mRNA dynamics depends on the mechanistic details, which can be translational repression, translational stimulation or mRNA degradation. Figure 3H shows the maximum sensitivity s_m in the parameter space spanned by the degradation rate constant β_{R1} and the translation rate constant α_{P1} of the mRNA–miRNA complex. In the blue region located in right-bottom corner, $s_m < -1$; thus, regulation of mRNA by miRNA shows different degrees of ultrasensitivity. Thus, in this region, a small n_{min} is sufficient to generate bistability (Fig. 3I). In the green region $-1 < s_m < 0$; thus, only subsensitivity can be obtained and n_{min} needs to be larger than 2. In this region, n_{min} may need to be larger than 2 to generate bistability. In the orange region, $s_m > 0$, the regulation of mRNA by miRNA shows subsensitive stimulation, which largely originates from the stimulation of translation of mRNA as a result of forming a complex with miRNA. It is noted that, in the subsensitive stimulation region, bistability cannot be generated. Taken together, the regulation of mRNA by miRNA can comprise ultrasensitive or subsensitive inhibition, and subsensitive activation and the ultrasensitivity from the regulation of mRNA by miRNA can absolutely subserve the generation of bistability and the cell fate decision.

Competing endogenous RNAs amplify the ultrasensitivity of mRNA–miRNA mutual regulation and thus extend the bistable region

In the above analyses, the miRNA has only one target mRNA. However, miRNA typically targets multiple mRNAs [19,37]. For example, miR-200 targets both zeb2 and pten [38]. To examine the effect of ceRNAs on the regulation of mRNA/protein by miRNA, we expanded the model to include a ceRNA.

As shown in Fig. 4A, without ceRNA, $[mR]_t$ first decreases slowly with increasing α_{miR}, then the decrease accelerates after α_{miR} exceeds a threshold value so that more miRNA molecules are available to effectively inhibit mRNA. The response curve of [P] changes in the presence of ceRNA, and the change depends on the value of K_c, the ceRNA–miRNA binding constant. When $K_c << K_1$, ceRNA only manifests its effect at the level of [P] with large α_{miR} when its concentration is sufficiently high to compete with the target mRNA. On the other hand, when $K_c >> K_1$, at small values of α_{miR}, the target mRNA under interest is largely unaffected by the miRNA inhibition because the ceRNA binds most of the miRNA molecules, and then its amount drops suddenly after α_{miR} is sufficiently large so the miRNA molecules titrate out the ceRNA molecules. Consequently, the $\alpha_{miR} - [P]$ response curve first decreases then increases its sharpness with K_c, which is revealed by the $s_m(\alpha_{miR}-P)-K_c$ curve in Fig. 4B. That is, when the ceRNA–miRNA

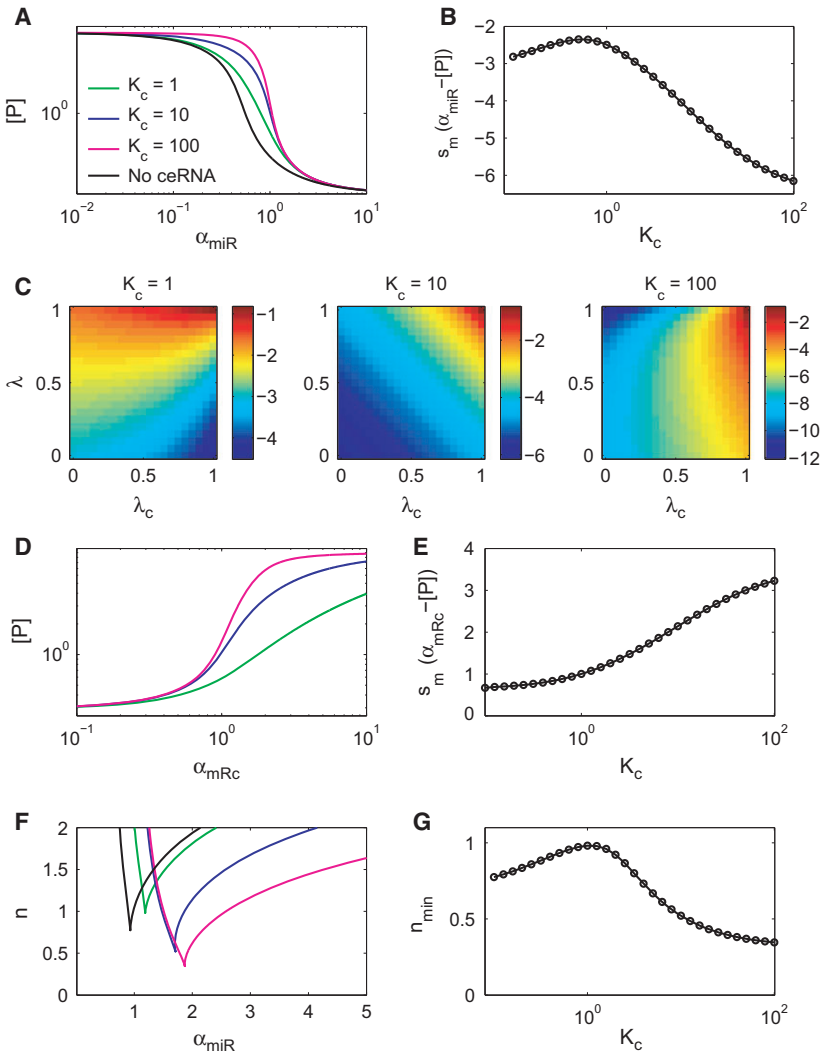

Fig. 4. Competitions between different mRNAs for a common type of miRNA affects the mRNA sensitivity to miRNA inhibition and bistability. Each mRNA is modeled with one miRNA binding site. (A) Response curves of the protein level ([P]) on the miRNA synthesis rate constant α_{miR} under different values of the ceRNA–miRNA binding constant K_c. The dashed line is the case without ceRNA. (B) The maximum sensitivity s_m of the α_{miR}–[P] response curve depends on the ceRNA-miRNA binding constant K_c. (C) Dependence of the maximum sensitivity s_m of the α_{miR} – [P] response curve on recycle ratios of the miRNA upon degradation of mRNA–miRNA complex (λ) and the ceRNA–miRNA complex (λ_c) under different ceRNA-miRNA binding constants. (D) Response curves of the protein level ([P]) on the ceRNA synthesis rate constant, α_{mRc}. (E) The maximum sensitivity s_m of the α_{mRc}–[P] curve depends on the ceRNA–miRNA binding constant. (F) Two-parameter bifurcation diagrams for α_{miR} versus n, respectively, with a different ceRNA–miRNA binding constant K_c. (G) The dependence of n_{min} on the ceRNA–miRNA binding constant K_c. $\lambda_c = 0.5$, $\alpha_{mRc} = 1$, $\beta_{mRc1} = 10$.

binding constant is small, ceRNA desensitizes the regulation of the mRNA by miRNA. However, after the binding constant exceeds a threshold, ceRNA sensitizes the regulation.

The above modulation of sensitivity, however, depends on the recycle ratios λ and λ_c. As shown in Fig. 4E, depending on K_c, the pattern of $s_m(\alpha_{miR}–P)$ in the space of λ and λ_c changes qualitatively. With $K_c < K_1$, for a fixed λ_c, $|s_m|$ decreases with an increased value of λ, which is consistent with that shown in Fig. 3. For a fixed λ, however, $|s_m|$ increases with λ_c. Especially when $\lambda_c \to 1$, the response becomes significantly more sensitive to miRNA inhibition. With $K_c = K_1$, $s_m(\alpha_{miR}–P)$ shows a linear anti-correlated dependence on λ and λ_c. This linear dependence turns out to be specific only when using the same parameter sets for the mRNA and the ceRNA, except the recycle ratios; otherwise, the results would be qualitatively similar to the case of $K_c < K_1$ or $K_c > K_1$. With $K_c > K_1$, the qualitative feature of the response is more or less the opposite of that with $K_c < K_1$, whereas the absolute value of s_m is much larger. For a fixed λ_c, $|s_m|$ initially decreases monotonically with an increasing value of λ, and then has an extremum at an intermediate value of λ when $\lambda_c \to 1$. For a fixed λ, $|s_m|$ instead decreases with λ_c. Despite difficulties in performing simple mathematical analyses, these results demonstrate that the presence of a ceRNA further complicates the dynamic behavior of mRNA–miRNA regulation.

Intuitively, a ceRNA provides certain protection of the target mRNA from miRNA inhibition through competitive binding of the latter. Indeed, Fig. 4D shows that ([P]) increases with the ceRNA synthesis rate constant α_{mRc}, and also shows positive sensitivity. Figure 4E shows that the sensitivity of this curve increases with K_c. Regulation of mRNA by ceRNA is subsensitive when ceRNA binding is weak (compared

to K_1) and ultrasensitive when ceRNA binding is strong. The response curve sensitivity also depends on the recycle ratio λ. As shown in Fig. S4A, $s_m(k_{mRc}-[P])$ increases with λ and K_c. Interestingly, the value of s_m does not change with λ_c except at the complete recycle point (Fig. S4B). Therefore, mRNAs can regulate each other indirectly by acting as a ceRNA of the other. This miRNA-mediated cross-talk tunes the sensitivity of mRNA–miRNA regulation. Several studies exist that have investigated the molecular determinants of effective ceRNA cross-talks [39–44], such as the miRNA/ceRNA ratio, numbers of total and shared miRNA response elements, and target binding affinity. However, the functionality of this increased sensitivity from ceRNA has not been studied previously. Thus, the minimum of Hill coefficient n_{min} for bistability is also analyzed by considering a ceRNA (Fig. 4F,G). n_{min} also first increases then decreases with K_c. That is, a ceRNA with high binding affinity can also contribute to the generation of bistability in the cell fate decision system. This is consistent with the non-monotonic dependence of s_m on K_c (Fig. 4B). Taken together, competing endogenous RNAs is able to amplify the ultrasensitivity of mRNA–miRNA mutual regulation and thus extend the bistable region.

Multiple miRNA binding sites on target mRNA lead to ultrasensitivity and bistability

In the above analyses, we modeled mRNAs with one miRNA binding site. Some mRNAs have multiple miRNA binding sites. For example, miR-200 can target to zeb1/2 mRNA on five or six highly conserved binding sites [45]. Thus, we systematically examined how the existence of two miRNA binding sites affect mRNA–miRNA mutual regulation and the generation of bistability.

Because there are two binding sites, there are two groups of possible mRNA–miRNA complexes, either with one miRNA bound (R_1) or two miRNAs bound (R_2) on mRNA. We denoted the recycle ratios of the two mRNA–miRNA complexes as λ_1 and λ_2, respectively. Figure 5A shows how the total mRNA level depends on the miRNA synthesis rate α_{miR} under different combinations of λ_1 and λ_2. Similar to the case for one binding site, the $\alpha_{miR}-[P]$ curve also shows ultrasensitivity and subsensitivity (Fig. 5A, cyan and magenta lines, respectively). More interestingly, by contrast to the response curve with one binding site, bistability occurs under the appropriate combination of λ_1 and λ_2 (Fig. 5A, black line). To the best of our knowledge, there is no previous report on bistability that results from the mutual regulation between miRNA and mRNA without any feedback loop. Future experiments can test this novel prediction by fine tuning the two recycle ratios.

To further explore how to generate specific response by tuning the recycle ratios, we locate bistable and monostable domains in the space of λ_1 and λ_2. As shown in Fig. 5B, bistability is generated in the corner where λ_1 is much smaller than λ_2 (blank region), whereas, in the other region, a different level of sensitivity is generated. The bistable–monostable boundary depends on other parameters. As shown in Fig. S5, the bistable regions can be expanded by increasing the mRNA–miRNA binding constant. The plausible underlying mechanism of bistability generated with multiple binding sites is that the formation of mRNA–$miRNA_2$ protects miRNA under large λ_2, whereas an increased level of miRNA promotes the formation of mRNA–miRNA then mRNA–$miRNA_2$ with ultrasensitivity under a smaller recycle ratio λ_1 (Fig. 3). This is equivalent to an inherent positive feedback loop with ultrasensitivity, meeting the requirement of bistability [36]. The reason why bistability cannot be generated from the one-binding site model is that the protective effect and ultrasensitivity cannot coexist simultaneously with one recycle ratio.

We further considered the involvement of the positive feedback loop and analyzed the contribution of mRNA–miRNA mutual regulation with multiple binding sites to bistability. We analyzed the dependence of n_{min} on the recycle ratios λ_1 or λ_2, respectively, with the other as a constant. First, with λ_2 fixed at 0.8 and a decrease of λ_1, the bistable region increases as the cusp point gradually decreases, as shown in the two-parameter bifurcation diagrams (Fig. 5C). Notably, as λ_1 is sufficiently small, the curve intersects with Hill coefficient boundary ($n = 0$). This is because such bistability can be generated directly from mRNA–miRNA mutual regulation with multiple binding sites without a positive feedback loop, as demonstrated in Fig. 5A,B. We use $n_{min} = 0$ to represent this intrinsic bistability. Overal, n_{min} increases with λ_1 (as shown in Fig. 5D). This is consistent with the dependence of n_{min} on the recycle ratio in the case of one binding site (Fig. 3F). However, the dependence of n_{min} on λ_2 is completely opposite. As shown in Fig. 5E,F, with constant $\lambda_1 = 0.8$, n_{min} decreases with λ_2. In addition, the effect of ceRNA on miRNA–mRNA mutual regulation is analyzed in the cases with two binding sites on mRNA or ceRNA, respectively, in Figs S6 and S7. In both cases, n_{min} first increases and then decreases with ceRNA–miRNA binding constant, with a trend similar to that shown in Fig. 4F, G. That is, a strong ceRNA

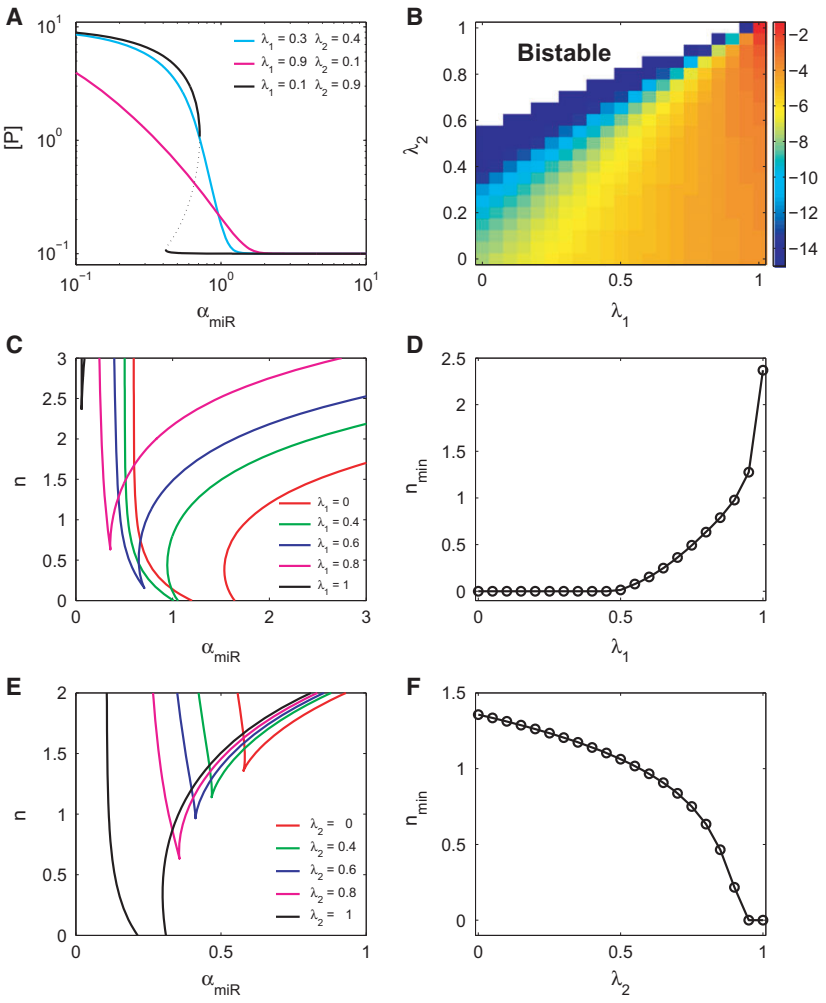

Fig. 5. Ultrasensitivity and bistability from multiple miRNA binding sites on one mRNA molecule. (A) Response curves of [P] on the miRNA synthesis rate constant α_{miR} under different combinations of the miRNA recycle ratios upon degradation of complex mNRA–miRNA (λ_1) and mRNA - miRNA$_2$ (λ_2). Dotted line denotes unstable states. (B) The maximum sensitivity $s_m(\alpha_{miR} - [P])$ in the space of λ_1 and λ_2. The space is divided into bistable (blank region) and monostable (with different sensitivity indicated by heatmap) regions. (C) Two-parameter bifurcation diagrams for α_{miR} versus n with different levels of λ_1 under constant $\lambda_2 = 0.8$. (D) The dependence of n_{min} on λ_1. (E) Two-parameter bifurcation diagrams for α_{miR} versus n with different levels of λ_2 under constant $\lambda_1 = 0.8$. (F) The dependence of n_{min} on λ_2. $d_{mR2} = 10$ and $K_1 = K_2 = 100$.

also could expand the bistability region in the case of multiple binding sites.

In summary, the reciprocal regulation between mRNA and miRNA is more versatile with two binding sites than with one binding site. A bistable switch has a greater possibility of existing in the mRNA–miRNA system with multiple binding sites. It would be interesting to carry out a similar analysis on the mRNA–miRNA systems with more than two binding sites, such as the miR-200/zeb1/2 system in which five or six binding sites are highly conserved [45].

Discussion

It is generally suggested that regulatory miRNAs serve as rheostats to fine-tune the expression of the target to accommodate cell responses [46,47]. In the present study, we systematically analyzed mutual regulation between miRNA and mRNA with a class of basic mathematical models. Unexpectedly, we found that this reciprocal regulation gives rise to rich dynamic features, which play important roles in the regulation of cellular processes such as cell phenotype change and maintenance.

mRNA–miRNA regulation provides a new mechanism for ultrasensitivity and bistability

The dynamics of a biological system is typically nonlinear. The nonlinearity results from a large variety of sources [48,49], such as cooperativity [50], homo-multimerization [51], zero-order ultrasensitivity [52], multisite phosphorylation [53,54], substrate competition [55], lateral interaction [27] and molecular titration [28]. Bistable and multistable switches are often involved in cell fate decisions in biological systems [26,56,57]. Reports show that miRNA regulation of mRNAs contributes to the robustness of a biological system when considering feedback or feedforward

loops [58–60]. Indeed, our analyses demonstrate that miRNA/mRNA reciprocal regulation is also a source of nonlinearity. It shows ultrasensitive and subsensitive inhibition, as well as subsensitive protection. This nonlinearity can contribute to the generation of a bistable switch and cell fate decisions in a biological system.

Positive feedback and ultrasensitivity are two prerequisites for bistability. In the present study, we showed that bistability is generated when ultrasensitivity from the mRNA–miRNA reciprocal regulation is equipped with a positive feedback loop. Furthermore, bistability also can be generated from mRNA–miRNA reciprocal regulation when more than one miRNA binding site exists in the absence of any imposed feedback regulation. This result is analogous to the bistability from multisite phosphorylation [61,62]. However, the underlying mechanisms of bistability are different for multisite mRNA–miRNA reciprocal regulation and multisite phosphorylation. The former results from the coexistence of ultrasensitivity and miRNA protection, whereas the later arises from substrate saturation and competitive inhibition [61].

mRNA–miRNA regulation provides mechanism for pathway cross-talks

Because there are typically multiple targets for a single miRNA, mRNAs can cross-regulate each other by competing for the shared miRNAs [38,39,43]. Thus, miRNAs link individual signaling pathways and form an intertwined ceRNA network (ceRNETs) [63]. Taking the ceRNETs into account makes the overall regulatory network more complex and leads us to rethink our view of the design principles of biological networks. The coupling of our model with other bio-networks, such as a protein–protein interaction network, metabolic network and gene regulatory network, will give more interesting dynamic phenomena. In addition, the design of miRNA sponges should take into consideration the potential effect of ceRNAs on a gene regulation network with miRNA involved. In the present study, we found that the bistable region is expanded because a larger degree of ultrasensitivity can be achieved when a stronger ceRNA is involved. Thus, this feature can be taken advantage of when designing more effective miRNA sponges.

Thermodynamic and kinetic parameters control dynamic features of mRNA–miRNA regulation

The versatile dynamics of mRNA–miRNA regulation results from interplay among a number of thermodynamic and kinetic parameters. For example, in the present study, we discussed how varying the miRNA recycle ratio alone can qualitatively change the regulation dynamics. It is already known that miRNAs can shield from exonucleolytic degradation by interacting with its target [14,64]. The underlying molecular mechanism is not well understood. It is suggested that target mRNA keeps miRNA bound with the Argonaute protein, protecting it from degradation [14]. Furthermore, it is implied that the extent of protection is positively correlated with the number of available target sites [11,64]. In the present study, we showed how this molecular-level detail manifests itself in the context of the network-level mRNA–miRNA regulation dynamics.

Quantitative measurements can test model predictions

It is unexpected that a simple mRNA-miRNA motif, with only one or two miRNA binding sites and possibly the presence of just one ceRNA, can generate such diverse dynamics by varying a few controlling parameters. Further studies may likely reveal even richer dynamics when the module is placed in the context of the global network dynamics and cell regulation, where multiple RNAs with different numbers of miRNA binding sites compete for common miRNAs. Given the varying copy numbers of both miRNAs and mRNAs [37], the consequence of stochasticity, which is not discussed in the present study, is another important topic to be explored. An open question is whether cells have explored and utilized all these theoretical possibilities, or whether functional requirements have converged the parameters to specific regions of the multi-dimensional parameter space.

To address the above question, it is necessary to achieve quantitative characterization of both thermodynamic and kinetic parameters of mRNA–miRNA regulation. The task is challenging but has been carried out to a certain extent. For example, it has been shown experimentally that miRNA is multiple-turnover, enabling several rounds of target recognition and cleavage per miRNA [18,65,66]. Mathematically, the number of rounds of target recognition and cleavage per miRNA, N_{round}, is related to the recycle ratio λ, satisfying $N_{\mathrm{round}} = 1/(1-\lambda)$. Therefore, λ can be estimated from the measured N_{round}. For example, when each human let-7-containing complex directs, on average, 10 rounds of mRNA cleavage [65], whereas each human miR-233 molecule regulates at least two target mRNA molecules [18], then the corresponding values of λ are 0.9 and 0.5, respectively. Haley and Zamore [66] showed that a let-7 small interfering RNA-directed

ribonucleoprotein complex catalyzes more than 50 target RNA cleavages (i.e. $\lambda > 0.98$). The extent of the complementary between miRNA and mRNA may also provide a clue about the value of λ. That is, the free energy of mRNA–miRNA binding is another factor controlling the recycle ratio. Accordingly, a specific miRNA can then be designed with a certain recycle ratio according to the degree of complementary that achieves the desired sensitivity. Combined computational structural modeling and experimental efforts may further accelerate the process.

mRNA–miRNA regulation dynamics needs to be explored at the level of network dynamics. Mukherji *et al*. [6] demonstrated the ultrasensitivity of miRNA-mediated regulation of mRNA, which results from molecular titration [28]. Similar quantitative measurements, together with synthetic designs that can modify various thermodynamic and kinetic parameters, are able to test the predictions made in the present study, such as the tunability of ultrasensitivity by controlling the recycle ratio. It is noted that polymorphism in miRNAs and their target sites may provided more variation for miRNA–mRNA binding and thus the recycle ratio. Integration of the information from PolymiRTS database [67] with our model analysis can enable additional insights to the functional variation of miRNA in physiological and pathological phenotypes.

In summary, mRNA–miRNA mutual regulation can generate versatile dynamics. A detailed understanding of the mechanistic details and functional roles of such regulation requires consorted efforts from quantitative measurements and computational analyses conducted at both the molecular and system levels. As mRNA–miRNA regulation prevalently exists in various biological systems and some of them function as a 'hub' to coordinately regulate others [68], the versatile effects of mRNA–miRNA reciprocal regulation have evolved to adapt to the specific biological context and it is robust to intrinsic and extrinsic noise. Thus, understanding the functionality of mRNA–miRNA in the biological system is critical for clarifying its underlying design principle.

Acknowledgements

We thank Dr Bing Liu for helpful discussions. The research was supported by the US National Science Foundation (Grant DMS-1462049).

Author contributions

X-JT and JX conceived and designed the study. X-JT performed the simulation. X-JT, HZ, JZ and JX analyzed the data. X-JT and JX wrote the paper. HZ and JZ helped with constructive discussion. All authors read and approved the manuscript submitted for publication.

References

1 Leonardo TR, Schultheisz HL, Loring JF and Laurent LC (2012) The functions of microRNAs in pluripotency and reprogramming. *Nat Cell Biol* **14**, 1114–1121.
2 Lamouille S, Subramanyam D, Blelloch R and Derynck R (2013) Regulation of epithelial-mesenchymal and mesenchymal-epithelial transitions by microRNAs. *Curr Opin Cell Biol* **25**, 200–207.
3 Sun X, Jiao X, Pestell TG, Fan C, Qin S, Mirabelli E, Ren H and Pestell RG (2014) MicroRNAs and cancer stem cells: the sword and the shield. *Oncogene* **33**, 4967–4977.
4 Pencheva N and Tavazoie SF (2013) Control of metastatic progression by microRNA regulatory networks. *Nat Cell Biol* **15**, 546–554.
5 Krol J, Loedige I and Filipowicz W (2010) The widespread regulation of microRNA biogenesis, function and decay. *Nat Rev Genet* **11**, 597–610.
6 Mukherji S, Ebert MS, Zheng GXY, Tsang JS, Sharp PA and van Oudenaarden A (2011) MicroRNAs can generate thresholds in target gene expression. *Nat Genet* **43**, 854–U60.
7 Huntzinger E and Izaurralde E (2011) Gene silencing by microRNAs: contributions of translational repression and mRNA decay. *Nat Rev Genet* **12**, 99–110.
8 Chekulaeva M and Filipowicz W (2009) Mechanisms of miRNA-mediated post-transcriptional regulation in animal cells. *Curr Opin Cell Biol* **21**, 452–460.
9 Chen XM (2009) Small RNAs and their roles in plant development. *Annu Rev Cell Dev Biol* **25**, 21–44.
10 Zamore PD, Tuschl T, Sharp PA and Bartel DP (2000) RNAi: double-stranded RNA directs the ATP-dependent cleavage of mRNA at 21 to 23 nucleotide intervals. *Cell* **101**, 25–33.
11 Pasquinelli AE (2012) MicroRNAs and their targets: recognition, regulation and an emerging reciprocal relationship. *Nat Rev Genet* **13**, 271–282.
12 Kai ZS and Pasquinelli AE (2010) MicroRNA assassins: factors that regulate the disappearance of miRNAs. *Nat Struct Mol Biol* **17**, 5–10.
13 Ruegger S and Grosshans H (2012) MicroRNA turnover: when, how, and why. *Trends Biochem Sci* **37**, 436–446.
14 Chatterjee S and Grosshans H (2009) Active turnover modulates mature microRNA activity in *Caenorhabditis elegans*. *Nature* **461**, 546–549.
15 Ameres SL, Horwich MD, Hung JH, Xu J, Ghildiyal M, Weng Z and Zamore PD (2010) Target RNA-directed trimming and tailing of small silencing RNAs. *Science* **328**, 1534–1539.

16 Cazalla D, Yario T and Steitz JA (2010) Down-regulation of a host microRNA by a *Herpesvirus saimiri* noncoding RNA. *Science* **328**, 1563–1566.
17 Ameres SL and Zamore PD (2013) Diversifying microRNA sequence and function. *Nat Rev Mol Cell Biol* **14**, 475–488.
18 Baccarini A, Chauhan H, Gardner TJ, Jayaprakash AD, Sachidanandam R and Brown BD (2011) Kinetic analysis reveals the fate of a microRNA following target regulation in mammalian cells. *Curr Biol* **21**, 369–376.
19 Bartel DP (2009) MicroRNAs: target recognition and regulatory functions. *Cell* **136**, 215–233.
20 Tay Y, Rinn J and Pandolfi PP (2014) The multilayered complexity of ceRNA crosstalk and competition. *Nature* **505**, 344–352.
21 Salmena L, Poliseno L, Tay Y, Kats L and Pandolfi PP (2011) A ceRNA hypothesis: the Rosetta Stone of a hidden RNA language? *Cell* **146**, 353–358.
22 Krek A, Grun D, Poy MN, Wolf R, Rosenberg L, Epstein EJ, MacMenamin P, da Piedade I, Gunsalus KC, Stoffel M *et al.* (2005) Combinatorial microRNA target predictions. *Nat Genet* **37**, 495–500.
23 Siemens H, Jackstadt R, Hünten S, Kaller M, Menssen A, Götz U and Hermeking H (2011) miR-34 and SNAIL form a double-negative feedback loop to regulate epithelial-mesenchymal transitions. *Cell Cycle* **10**, 4256–4271.
24 Yamakuchi M and Lowenstein CJ (2009) MiR-34, SIRT1 and p53: the feedback loop. *Cell Cycle* **8**, 712–715.
25 Rokavec M, Oner MG, Li H, Jackstadt R, Jiang L, Lodygin D, Kaller M, Horst D, Ziegler PK, Schwitalla S *et al.* (2014) IL-6R/STAT3/miR-34a feedback loop promotes EMT-mediated colorectal cancer invasion and metastasis. *J Clin Invest* **124**, 1853–1867.
26 Tian X-J, Zhang H and Xing J (2013) Coupled reversible and irreversible bistable switches underlying TGFbeta-induced epithelial to mesenchymal transition. *Biophys J* **105**, 1079–1089. (First mathematical model for EMT).
27 Zhang H, Tian X-J, Mukhopadhyay A, Kim KS and Xing J (2014) Statistical mechanics model for the dynamics of collective epigenetic histone modification. *Phys Rev Lett* **112**, 068101.
28 Buchler NE and Louis M (2008) Molecular titration and ultrasensitivity in regulatory networks. *J Mol Biol* **384**, 1106–1119.
29 Lu M, Jolly MK, Levine H, Onuchic JN and Ben-Jacob E (2013) MicroRNA-based regulation of epithelial-hybrid-mesenchymal fate determination. *Proc Natl Acad Sci USA* **110**, 18144–18149.
30 Osella M, Riba A, Testori A, Cora D and Caselle M (2014) Interplay of microRNA and epigenetic regulation in the human regulatory network. *Front Genet* **5**, 345.
31 Bu P, Chen KY, Chen JH, Wang L, Walters J, Shin YJ, Goerger JP, Sun J, Witherspoon M, Rakhilin N *et al.* (2013) A microRNA miR-34a-regulated bimodal switch targets Notch in colon cancer stem cells. *Cell Stem Cell* **12**, 602–615.
32 Zhou P, Cai S, Liu Z and Wang R (2012) Mechanisms generating bistability and oscillations in microRNA-mediated motifs. *Phys Rev E Stat Nonlin Soft Matter Phys* **85** (4 Pt 1), 041916.
33 Savageau MA (1976) *Biochemical Systems Analysis: A Study of Function and Design in Molecular Biology*. Addison-Wesley, Reading, MA.
34 Liu B and Thiagarajan PS (2012) Modeling and analysis of biopathways dynamics. *J Bioinform Comput Biol* **10**, 1231001.
35 Clewley R (2012) Hybrid models and biological model reduction with PyDSTool. *PLoS Comput Biol* **8**, e1002628.
36 Angeli D, Ferrell JE Jr and Sontag ED (2004) Detection of multistability, bifurcations, and hysteresis in a large class of biological positive-feedback systems. *Proc Natl Acad Sci USA* **101**, 1822–1827.
37 Bartel DP (2004) MicroRNAs: genomics, biogenesis, mechanism, and function. *Cell* **116**, 281–297.
38 Karreth FA, Tay Y, Perna D, Ala U, Tan SM, Rust AG, DeNicola G, Webster KA, Weiss D, Perez-Mancera PA *et al.* (2011) In vivo identification of tumor- suppressive PTEN ceRNAs in an oncogenic BRAF-induced mouse model of melanoma. *Cell* **147**, 382–395.
39 Ala U, Karreth FA, Bosia C, Pagnani A, Taulli R, Leopold V, Tay Y, Provero P, Zecchina R and Pandolfi PP (2013) Integrated transcriptional and competitive endogenous RNA networks are cross-regulated in permissive molecular environments. *Proc Natl Acad Sci USA* **110**, 7154–7159.
40 Figliuzzi M, Marinari E and De Martino A (2013) MicroRNAs as a selective channel of communication between competing RNAs: a steady-state theory. *Biophys J* **104**, 1203–1213.
41 Figliuzzi M, De Martino A and Marinari E (2014) RNA-based regulation: dynamics and response to perturbations of competing RNAs. *Biophys J* **107**, 1011–1022.
42 Bosia C, Pagnani A and Zecchina R (2013) Modelling competing endogenous RNA networks. *PLoS One* **8**, e66609.
43 Yuan Y, Liu B, Xie P, Zhang MQ, Li YD, Xie Z and Wang XW (2015) Model-guided quantitative analysis of microRNA-mediated regulation on competing endogenous RNAs using a synthetic gene circuit. *Proc Natl Acad Sci USA* **112**, 3158–3163.
44 Bosson AD, Zamudio JR and Sharp PA (2014) Endogenous miRNA and target concentrations determine susceptibility to potential ceRNA competition. *Mol Cell* **56**, 347–359.

45 Brabletz S and Brabletz T (2010) The ZEB/miR-200 feedback loop[mdash]a motor of cellular plasticity in development and cancer? *EMBO Rep* **11**, 670–677.
46 Selbach M, Schwanhausser B, Thierfelder N, Fang Z, Khanin R and Rajewsky N (2008) Widespread changes in protein synthesis induced by microRNAs. *Nature* **455**, 58–63.
47 Baek D, Villen J, Shin C, Camargo FD, Gygi SP and Bartel DP (2008) The impact of microRNAs on protein output. *Nature* **455**, 64–71.
48 Novák B and Tyson JJ (2008) Design principles of biochemical oscillators. *Nat Rev Mol Cell Biol* **9**, 981–991.
49 Zhang Q, Bhattacharya S and Andersen ME (2013) Ultrasensitive response motifs: basic amplifiers in molecular signalling networks. *Open Biol* **3**, 130031.
50 Ferrell J (2009) Q&A: cooperativity. *J Biol* **8**, 53.
51 Notides AC, Lerner N and Hamilton DE (1981) Positive cooperativity of the estrogen receptor. *Proc Natl Acad Sci USA* **78**, 4926–4930.
52 Goldbeter A and Koshland DE Jr (1981) An amplified sensitivity arising from covalent modification in biological systems. *Proc Natl Acad Sci USA* **78**, 6840–6844.
53 Gunawardena J (2005) Multisite protein phosphorylation makes a good threshold but can be a poor switch. *Proc Natl Acad Sci USA* **102**, 14617–14622.
54 Ferrell JE Jr and Ha SH (2014) Ultrasensitivity part II: multisite phosphorylation, stoichiometric inhibitors, and positive feedback. *Trends Biochem Sci* **39**, 556–569.
55 Kim SY and Ferrell JE Jr (2007) Substrate competition as a source of ultrasensitivity in the inactivation of Wee1. *Cell* **128**, 1133–1145.
56 Tian X-J, Zhang XP, Liu F and Wang W (2009) Interlinking positive and negative feedback loops creates a tunable motif in gene regulatory networks. *Phys Rev E Stat Nonlin Soft Matter Phys* **80** (1 Pt 1), 011926.
57 Hong T, Watanabe K, Ta CH, Villarreal-Ponce A, Nie Q and Dai X (2015) An Ovol2-Zeb1 mutual inhibitory circuit governs bidirectional and multi-step transition between epithelial and mesenchymal states. *PLoS Comput Biol* **11**, e1004569.
58 Tsang J, Zhu J and van Oudenaarden A (2007) MicroRNA-mediated feedback and feedforward loops are recurrent network motifs in mammals. *Mol Cell* **26**, 753–767.
59 Ebert MS and Sharp PA (2012) Roles for microRNAs in conferring robustness to biological processes. *Cell* **149**, 515–524.
60 Osella M, Bosia C, Cora D and Caselle M (2011) The role of incoherent microRNA-mediated feedforward loops in noise buffering. *PLoS Comput Biol* **7**, e1001101.
61 Markevich NI, Hoek JB and Kholodenko BN (2004) Signaling switches and bistability arising from multisite phosphorylation in protein kinase cascades. *J Cell Biol* **164**, 353–359.
62 Ortega F, Garces JL, Mas F, Kholodenko BN and Cascante M (2006) Bistability from double phosphorylation in signal transduction. Kinetic and structural requirements. *FEBS J* **273**, 3915–3926.
63 Sanchez-Mejias A and Tay Y (2015) Competing endogenous RNA networks: tying the essential knots for cancer biology and therapeutics. *J Hematol Oncol* **8**, 30.
64 Chatterjee S, Fasler M, Bussing I and Grosshans H (2011) Target-mediated protection of endogenous microRNAs in *C. elegans*. *Dev Cell* **20**, 388–396.
65 Hutvagner G and Zamore PD (2002) A microRNA in a multiple-turnover RNAi enzyme complex. *Science* **297**, 2056–2060.
66 Haley B and Zamore PD (2004) Kinetic analysis of the RNAi enzyme complex. *Nat Struct Mol Biol* **11**, 599–606.
67 Bhattacharya A, Ziebarth JD and Cui Y (2014) PolymiRTS Database 3.0: linking polymorphisms in microRNAs and their target sites with human diseases and biological pathways. *Nucleic Acids Res* **42**, D86–D91.
68 Tsang JS, Ebert MS and van Oudenaarden A (2010) Genome-wide dissection of MicroRNA functions and cotargeting networks using gene set signatures. *Mol Cell* **38**, 140–153.

Supporting information

Additional Supporting Information may be found online in the supporting information tab for this article:

Fig. S1. Method of locating the minimum of Hill coefficient $n_{\min}$ to generate bistability.

Fig. S2. Nullclines of the total levels of protein and miRNA.

Fig. S3. Dependence of the maximum sensitivity s_m and minimal Hill coefficient $n_{\min}$ on other parameters.

Fig. S4. Dependence of the sensitivity of ceRNA-mediated regulation of mRNA on recycle ratios.

Fig. S5. Dependence of bistability boundary in the space of λ_1 and λ_2.

Fig. S6. Effect of ceRNA on the minimum of Hill coefficient $n_{\min}$ for bistability under the case with two miRNA binding sites on mRNA.

Fig. S7. Effect of ceRNA on the minimum of Hill coefficient $n_{\min}$ for bistability under the case with two miRNA binding sites on ceRNA.